3-10 SAR観測における電離層の影響 (セッション3: 地盤沈下, 地すべり, 観測・解析技術)

AUTHOR(S):

島田, 政信

CITATION:

島田, 政信. 3-10 SAR観測における電離層の影響 (セッション3: 地盤沈下, 地すべり, 観測・解析技術). SAR研究の新時代に向けて 2013: 共同研究（一般研究集会）24K-05.

ISSUE DATE:

2013-02

URL:

http://hdl.handle.net/2433/173589

3-10

SAR 観測における電離層の影響

島田政信

宇宙航空研究開発機構、地球観測研究センター、茨城県つくば市千現2−1−1、
tel:050-3362-4489, fax:029-868-2961, mail:shimada.masanobu@jaxa.jp

概要　2006年1月24日に打ち上げられた ALOS には、JERS-1 を継承する L-band SAR として、更に性能向上と高機能化を果たした PALSAR が搭載され、運用を通して、干渉処理技術の高度化のみならず、L-band SAR の有用性の認識と将来の向上に必要な課題が見えてきた。有用性としては、高い干渉性が確認されたこと、干渉性を用いたデータ利用研究が増えてきたこと、（地盤沈下、火山監視、地盤沈下、干渉性を用いた土地利用分類）、高度処理技術であるが時系列データ解析が増えてきたことである。一方、顕在化した課題としては電離層の認識とその取り扱いである。ある意味では、電離層監視手法の開発と同時に補正技術の解析が重要課題になってきた。本発表では、ALOS 運用開始から見られた電離層の現状とその補正の概要を紹介する（予定）。

SAR観測における電離層の影響

島田政信
JAXA/EORC
平成24年9月12、13日＠京大

Contents

- SARと電離層について
- 幾つかの実例
  - Faraday Rotation
  - TID
  - Streaking (Scintillation)
- 補正方法（の紹介。しかし、、、、）
- 将来の展望

Shisen
RSP124

ScanSAR : descending

DinSAR: Ascending

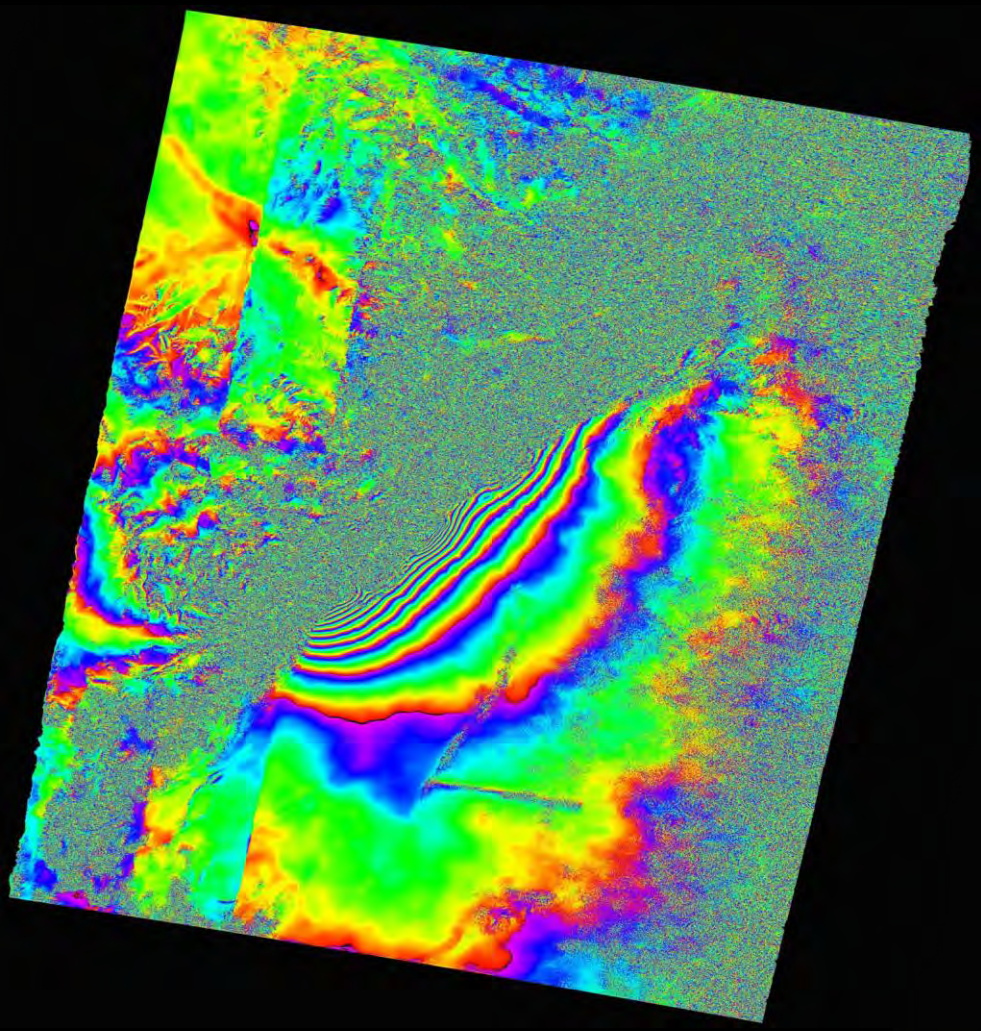

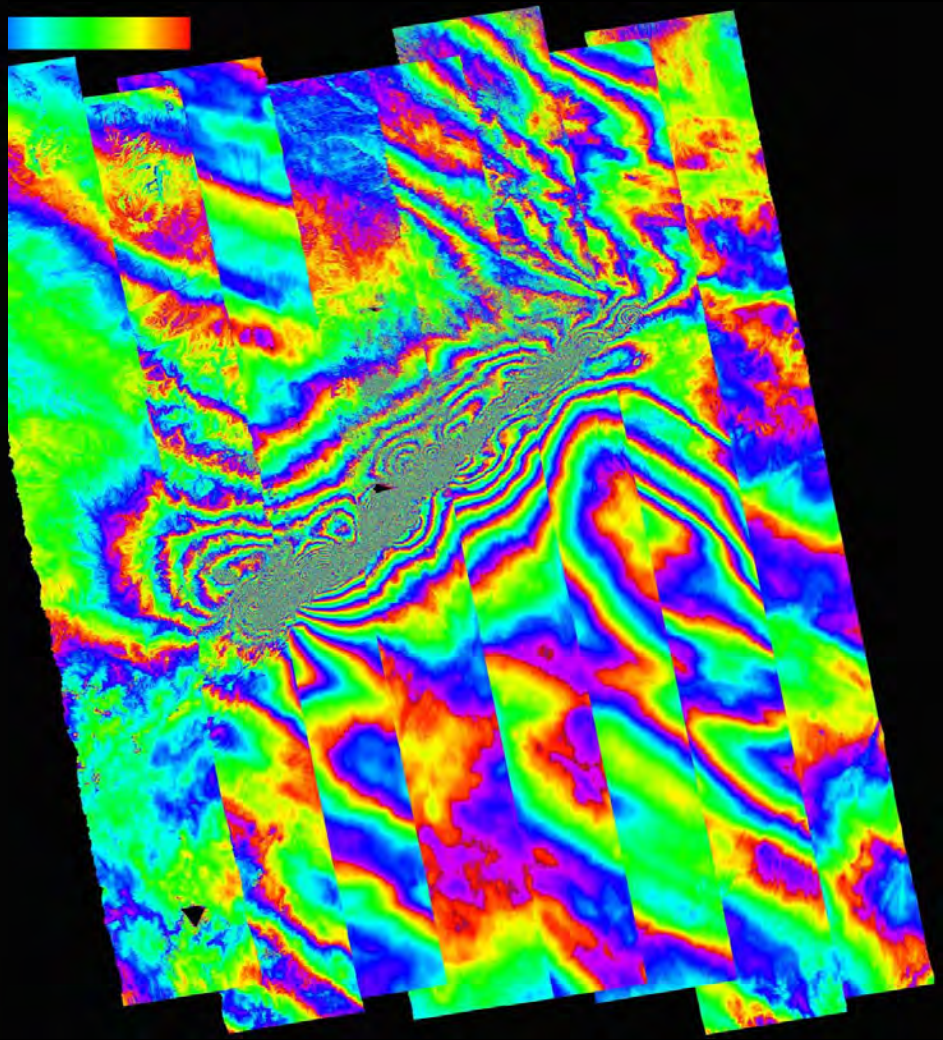

Amplitude image (hh polarization) 2006/11/05

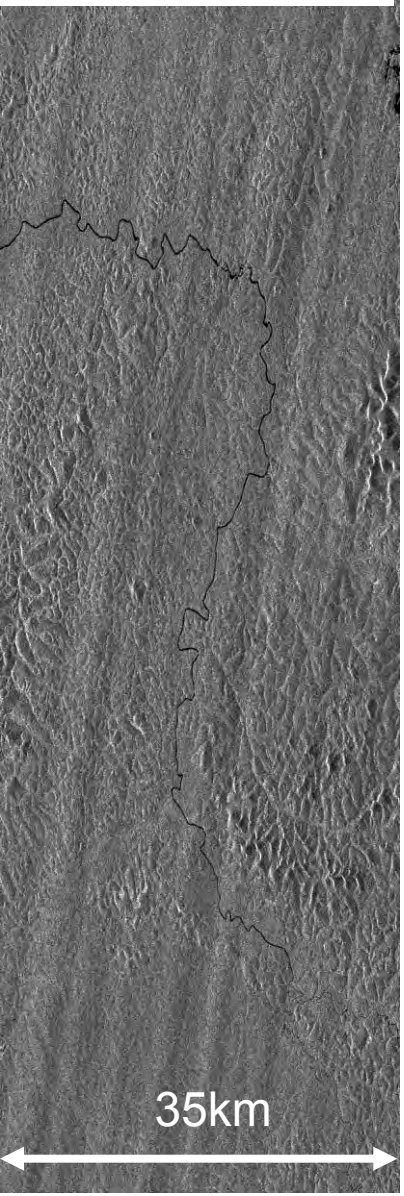

Phase (orbit and terrain corrected phase)

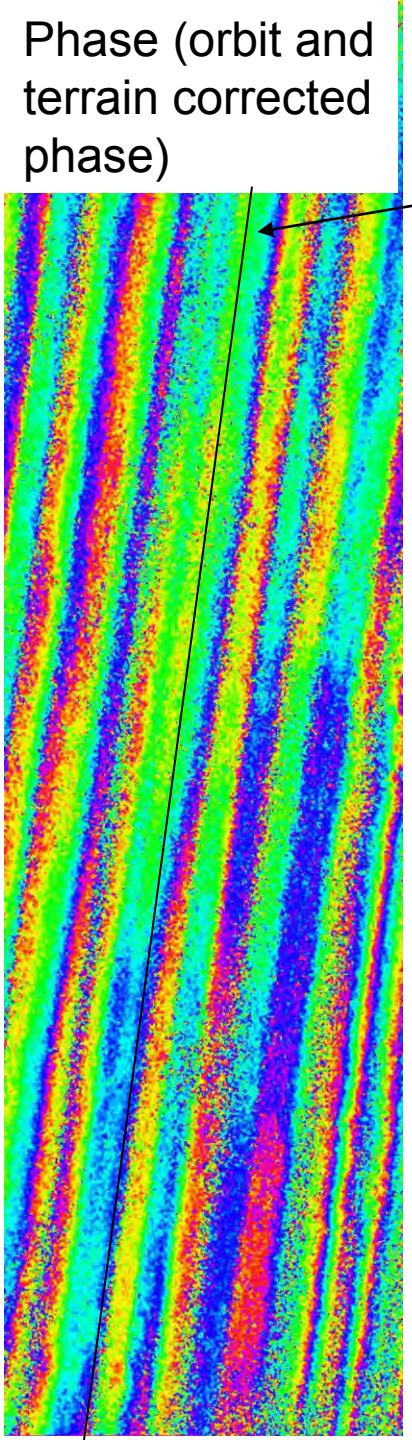

One example of lower latitude case in Brazil

Direction of the line

20060920-20061105:RSP072:Brazil

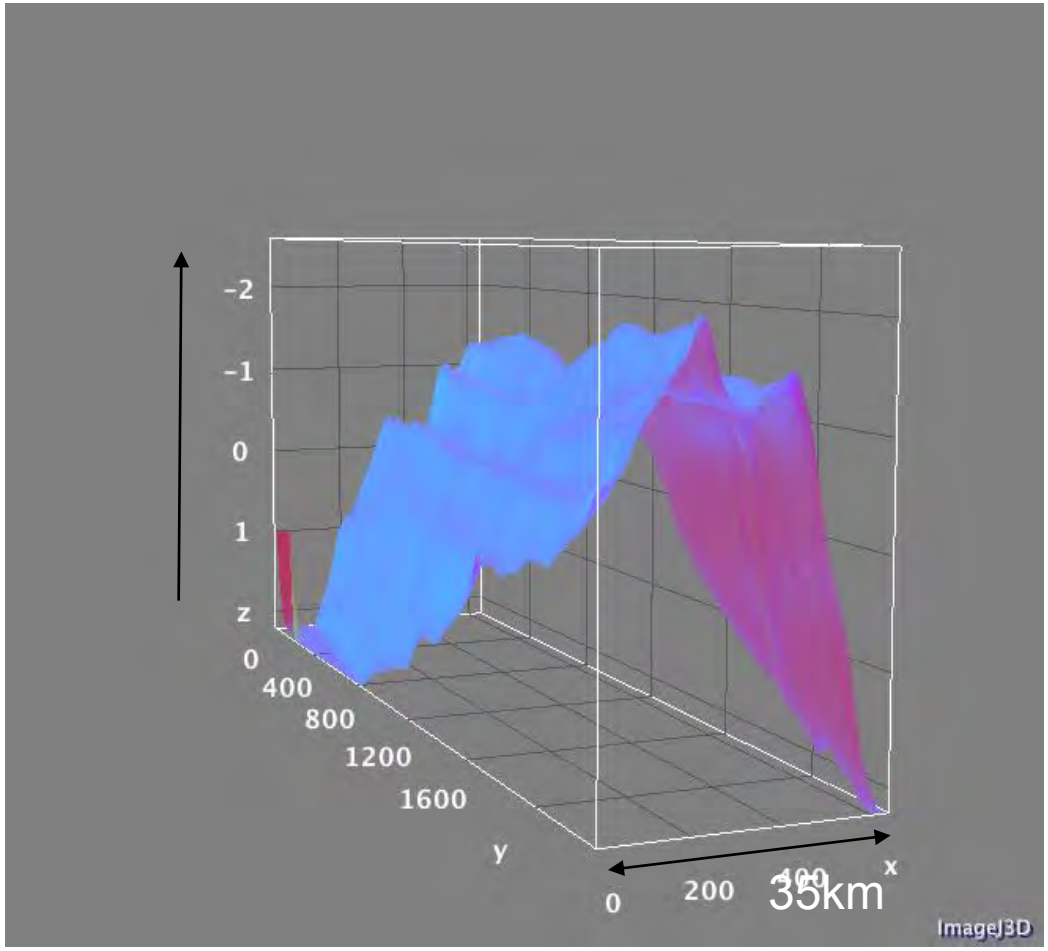

Unwrapped phase

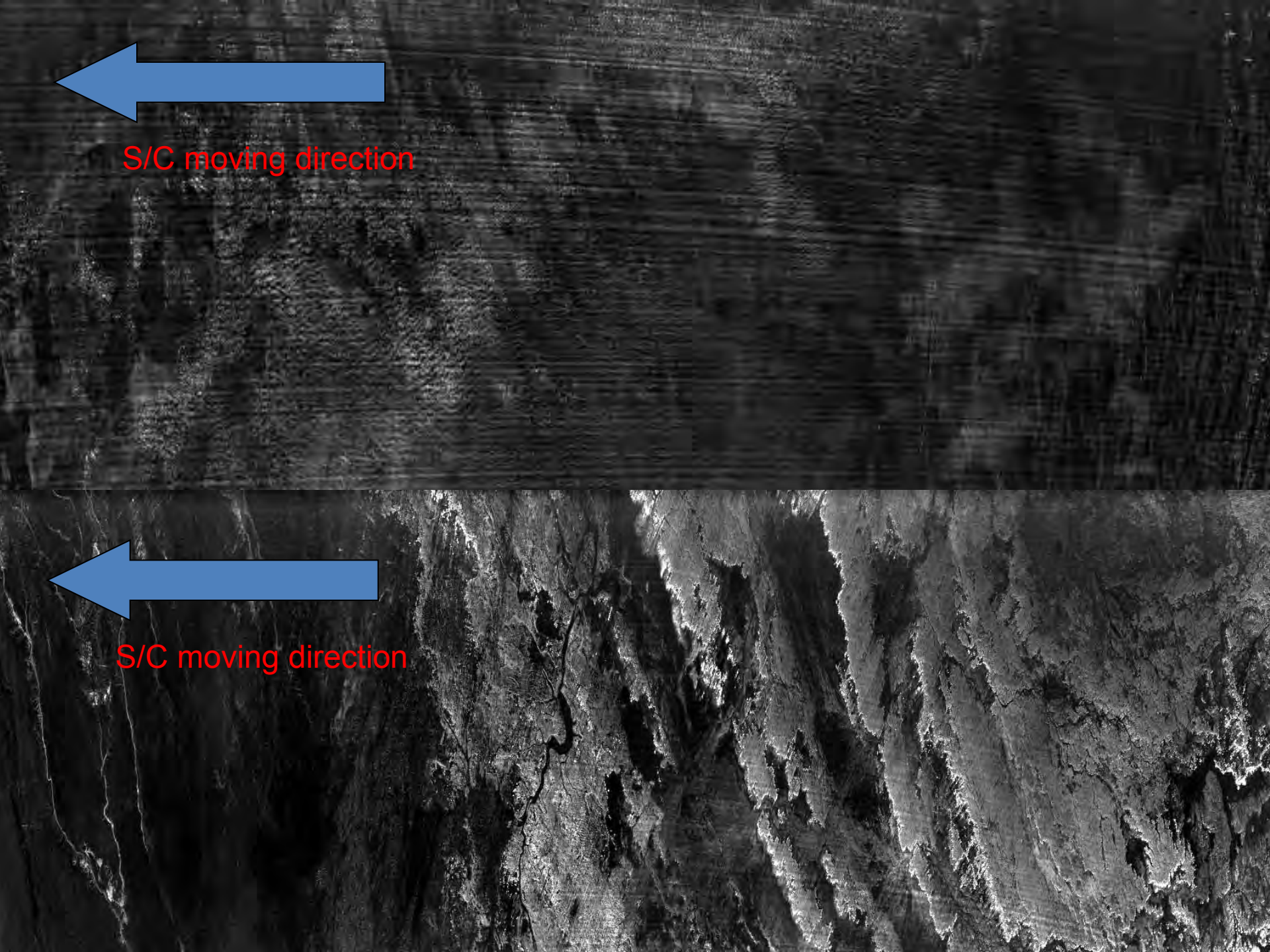
S/C moving direction
S/C moving direction

Siberia Area no.1

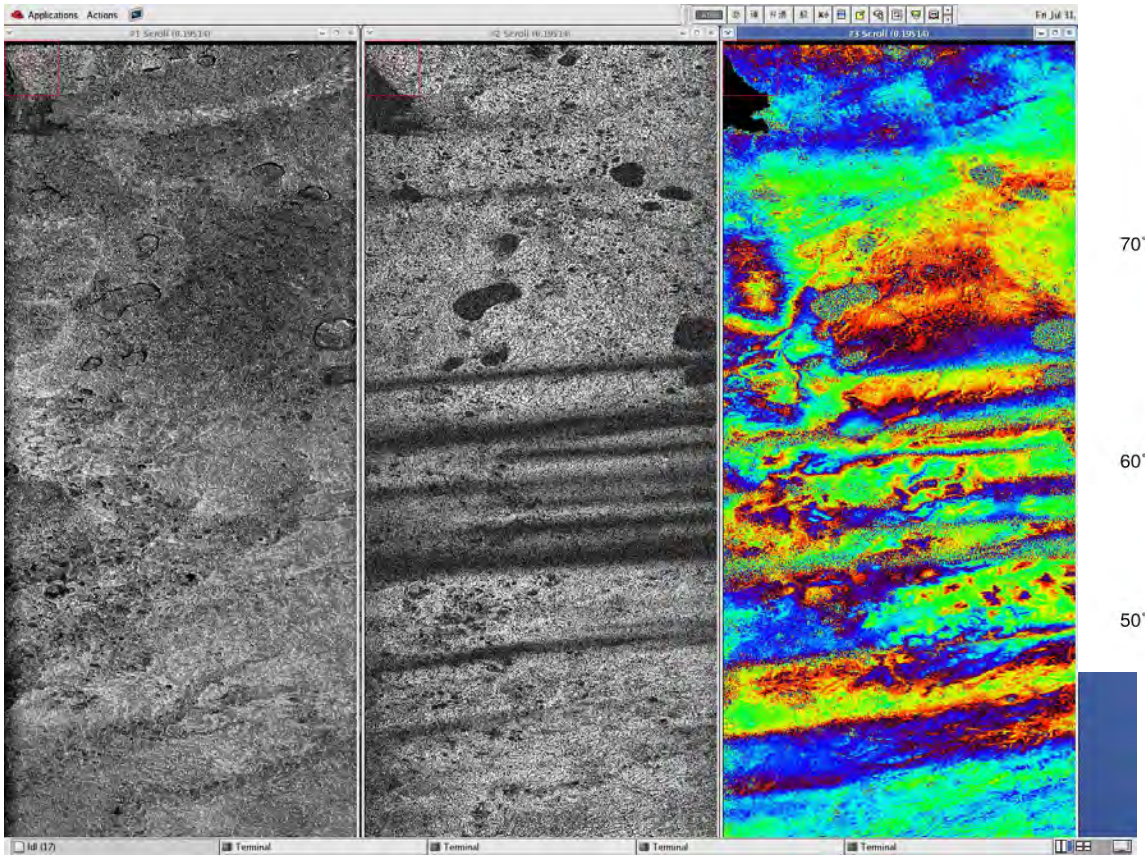

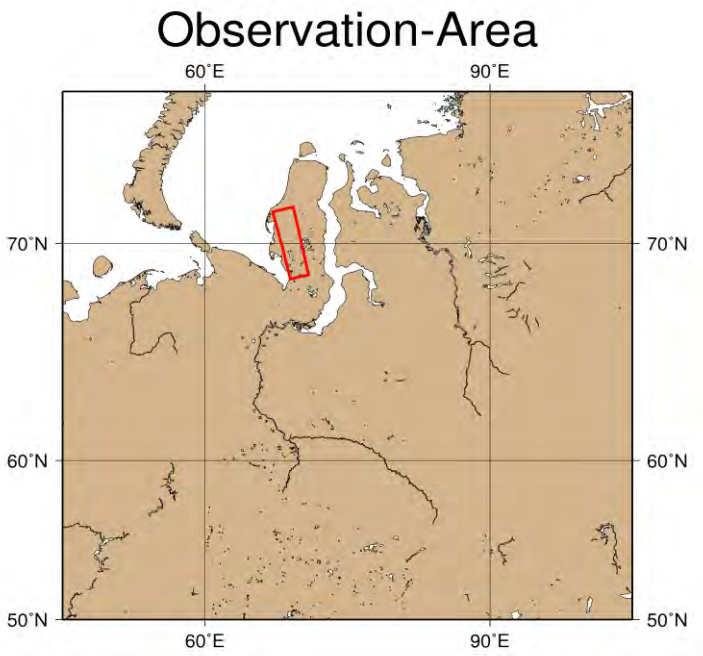

Four corner lat/lon

71.15N,67.14E 71.32N,69.28E
68.61N,69.00E 68.77N,70.90E

Master image(sar.p_m)
coherence(sar.corr)
DInSAR(sar.ddtma)

RSP: 516
Date: 2009/02/14(Master) W1118562001-01
2008/12/30(Slave) W1072516001-07
Bperp : 1550.9m
FBS343H - FBS343H
Ascending

Siberia 2

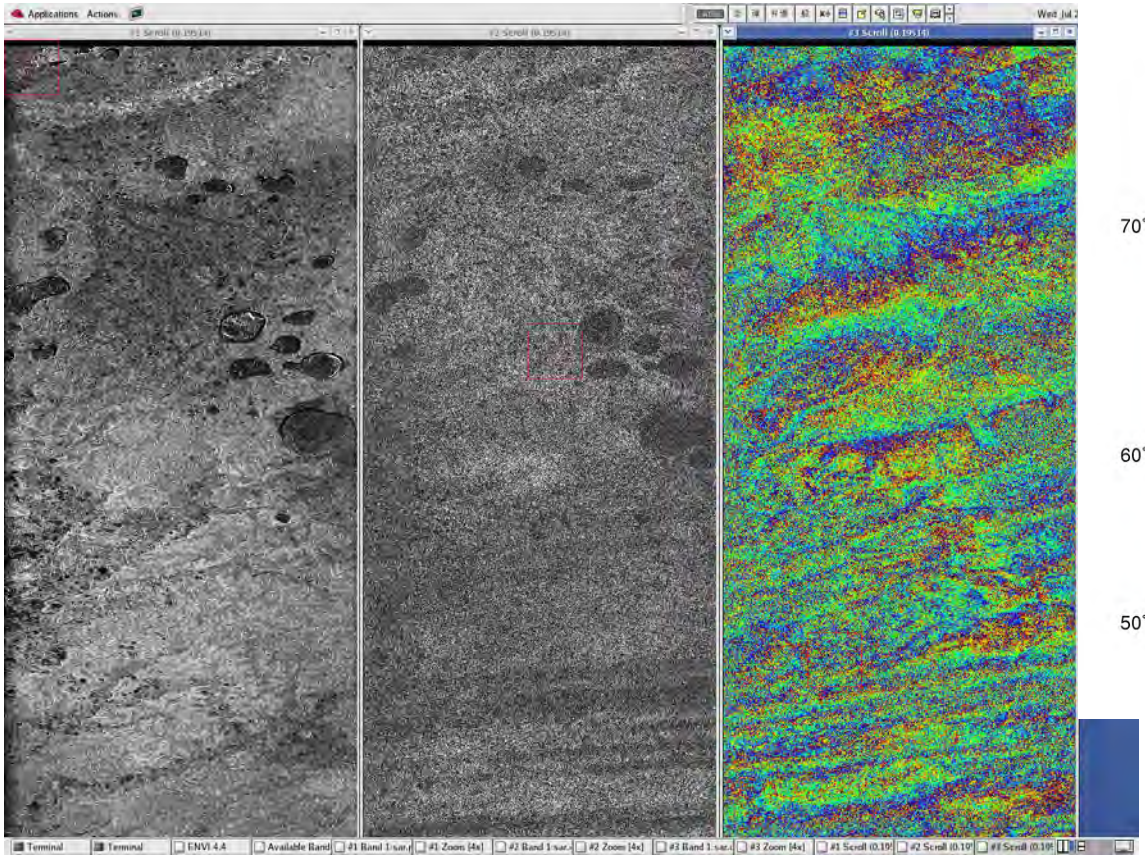

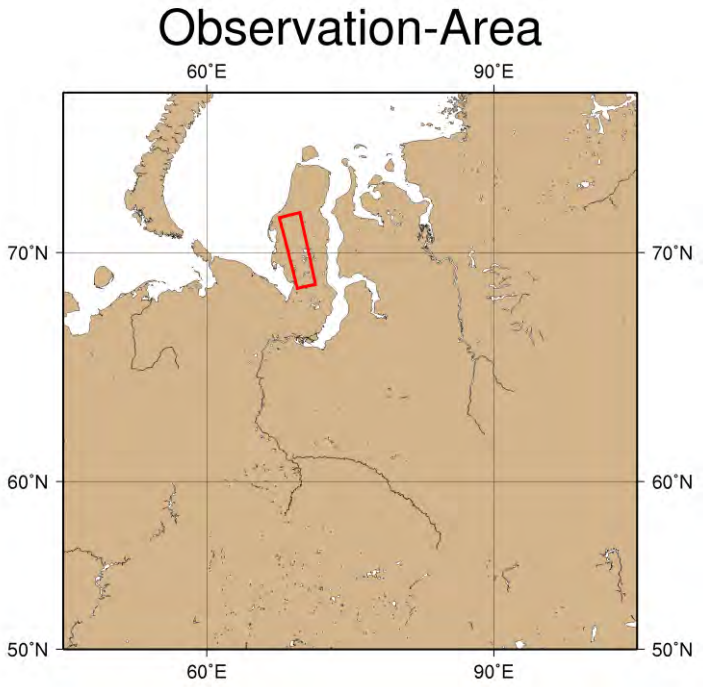

71.21N 67.62E 71.38N 69.77E
68.67N 69.49E 68.83N 71.39E

Master(sar.p_m)
coherence(sar.corr)
DinSAR(sar.ddtma)

RSP: 515
Date: 2009/01/28(Master) W1101515002-09
2008/10/28(Slave) W1009515001-03
Bperp: 1937.2m
FBS343H - FBS343H
Ascending

1. Disturbance at higher latitudes

Area	segments	Totals segments	Ratio(%)	Streaks in
Siberia	546 S (273)	1274 S (637)	42.9%	Coherence phase
Alaska	338 S (169)	2025 S(1012.5)	16.7%	Coherence and phase

2. Streaks at lower latitudes

Area	strips	Totals strips	Ratio(%)	Streaks in
Equatorial area	1490	64500	2.5%	Coherence phase

電離層、SAR画像への現れ方、補正方法

Items	Appearance	SAR	Method
Faraday Rotation	Orientation Rotation appeared in SLC	Polarimetry	BB
Scintillation	Streak Noise Location shift	Polarization Independency, Amplitude-phase	Fourier Correction-amplitude – not for location
TID or low frequency component in InSAR phase	Noise in phase or small azimuth shift	Polarization independency, Phase only	Model-based method Co-registration method Split-widow method

補正方法

- 振幅データ
  - 2D FFT方法：但し、位相量の補正は出来ない
- 位相データ
  - Split Window法（Rosen et al.)
  - Local Max-Coregistration 法（DLR）
  - Model法（Meyer et al.)
  - 一般に（非常に）難しい。成功例はないといっても過言でない。
- 偏波
  - BB法で補正出来る。

SARと電離層

$$S = F\left(-\frac{2}{l_0} n \times R \right) \oplus F_g$$

$$P_r = \frac{P_t G}{4\pi R^2} s^0 bR \frac{Ct}{2\cos q} \frac{Gl^2}{4\pi} \frac{1}{4\pi R^2} + P_n = \frac{P_t G^2 l^2}{(4\pi)^2 R^3} s^0 b \frac{Ct}{2\cos q} + P_n$$

$$P_C = A \frac{P_t G^2 l^2}{(4\pi)^2 R} s^0 b \frac{Ct}{2\cos q} + BP_n R$$

$$f$$

$$f = -\frac{4\pi}{l_0}\left(r_m n_m - r_s n_s \right)$$

$$= -\frac{4\pi}{l_0}\left(r_m n_m - r_s n_m + r_s n_m - r_s n_s \right)$$

$$= -\frac{4\pi}{l_0} n_m \left(r_m - r_s \right) - \frac{4\pi}{l_0} r_s \left(n_m - n_s \right)$$

$$= -\frac{4\pi}{l_0} n_m \left(\frac{B_{perp} z}{r_m \sin q} + B_{para} + dr \right) - \frac{4\pi}{l_0} r_s \left(n_m - n_s \right)$$

n：屈折率(Refractive Index)：

$$n = \sqrt{1 - \frac{Ne^2}{me_0\omega^2}}$$

$$n \approx 1 - \frac{1}{2}\frac{f_N^2}{f_0^2}\left(1 \mp \frac{f_H}{f_0}\cos\theta\right) - \frac{1}{8}\frac{f_N^4}{f_0^4} + ...(Appleton - Hartree\ equation)$$

2．ポラリメトリによるTEC推定

1. ポラリメトリによる解析：偏波面回転量とTECの関係

$$\begin{pmatrix} Z_{hh} & Z_{hv} \\ Z_{vh} & Z_{vv} \end{pmatrix} = A\frac{1}{r}e^{\frac{-4\rho r}{\lambda}} \begin{pmatrix} 1 & d_3 \\ d_4 & f_2 \end{pmatrix} \begin{pmatrix} \cos\Omega & \sin\Omega \\ -\sin\Omega & \cos\Omega \end{pmatrix}$$

$$\times \begin{pmatrix} S_{hh} & S_{hv} \\ S_{vh} & S_{vv} \end{pmatrix} \begin{pmatrix} \cos\Omega & \sin\Omega \\ -\sin\Omega & \cos\Omega \end{pmatrix} \begin{pmatrix} 1 & d_1 \\ d_2 & f_1 \end{pmatrix}$$

where $\mathbf{Z}_{ij}$ is the measurement matrix, i is the transmission polarization, j is the reception polarization, A is the amplitude, r is the slant range, **S**ij is the true scattering matrix of the target, $\mathbf{f}_1$ is the channel imbalance of the transmission distortion matrix, $\mathbf{f}_2$ is that for the reception matrix, ™$_1$ (™$_2$) are the cross talks of transmission, and ™$_3$ (™$_4$) are the those for the reception. Here, noise is ignored.

校正は森林とコーナー反射鏡を使用

Solutions are obtained by using Quegan's method and assuming $\Omega = 0$

Faraday Rotationの計算

手法は各種存在

$$\begin{pmatrix} \mathbf{Z}_{hh} & \mathbf{Z}_{hv} \\ \mathbf{Z}_{vh} & \mathbf{Z}_{vv} \end{pmatrix} = \begin{pmatrix} \cos\Omega & \sin\Omega \\ -\sin\Omega & \cos\Omega \end{pmatrix} \begin{pmatrix} \mathbf{S}_{hh} & \mathbf{S}_{hv} \\ \mathbf{S}_{vh} & \mathbf{S}_{vv} \end{pmatrix} \begin{pmatrix} \cos\Omega & \sin\Omega \\ -\sin\Omega & \cos\Omega \end{pmatrix}$$

1) $\mathbf{S}_{hv} = \mathbf{S}_{vh}$ $\quad \Omega = \frac{1}{2}\tan^{-1}\left(\frac{Z_{hv} - Z_{vh}}{Z_{hh} + Z_{vv}}\right)$ Freeman et al. ??

2) $\Omega = \frac{1}{4} Arg\left\langle Z_{LR} \times Z_{RL}^{*} \right\rangle$ $\quad \begin{pmatrix} \mathbf{Z}_{LL} & \mathbf{Z}_{LR} \\ \mathbf{Z}_{RL} & \mathbf{Z}_{RR} \end{pmatrix} = \begin{pmatrix} 1 & \mathbf{j} \\ \mathbf{j} & 1 \end{pmatrix} \begin{pmatrix} \mathbf{Z}_{hh} & \mathbf{Z}_{hv} \\ \mathbf{Z}_{vh} & \mathbf{Z}_{vv} \end{pmatrix} \begin{pmatrix} 1 & \mathbf{j} \\ \mathbf{j} & 1 \end{pmatrix}$

3) $\left\langle \mathbf{S}_{hv} \times \mathbf{S}_{hv}^{*} \right\rangle = \left\langle \mathbf{S}_{vh} \times \mathbf{S}_{vh}^{*} \right\rangle$

$$a = \left\langle (\mathbf{Z}_{hv} + \mathbf{Z}_{vh}) \times (\mathbf{Z}_{hh} + \mathbf{Z}_{vv})^{*} \right\rangle + \left\langle (\mathbf{Z}_{hv} + \mathbf{Z}_{vh})^{*} \times (\mathbf{Z}_{hh} + \mathbf{Z}_{vv}) \right\rangle$$

$$b = \left\langle \mathbf{Z}_{hv} \times \mathbf{Z}_{hv}^{*} - \mathbf{Z}_{vh} \times \mathbf{Z}_{vh}^{*} \right\rangle$$

$$\Omega_1 = \tan^{-1}\left\{ \frac{b}{a}\left(1 - \tan^4\Omega_0\right) - \tan^3\Omega_0 \right\}$$

$$a \times \tan\Omega\left(1 + \tan^2\Omega\right) - b\left(1 - \tan^4\Omega\right) = 0$$

$$\Omega_0 = \tan^{-1}\left(\frac{b}{a}\right)$$

Faraday Rotation Angel (model)

$$W = \frac{K}{f^2}\overline{B \times \cos\psi \times \sec\theta_0} \times TEC$$

where K=2.365x10^4 in SI units, f is the transmission frequency (Hz), TEC is the total electron contents (m^3/m^2), B is the geomagnetic flux density (Tesla), ψ is the angle between the geomagnetic field vector and the radar line-of-sight (radian), θ_0 the incidence angle, and the over-bars indicate averaging.

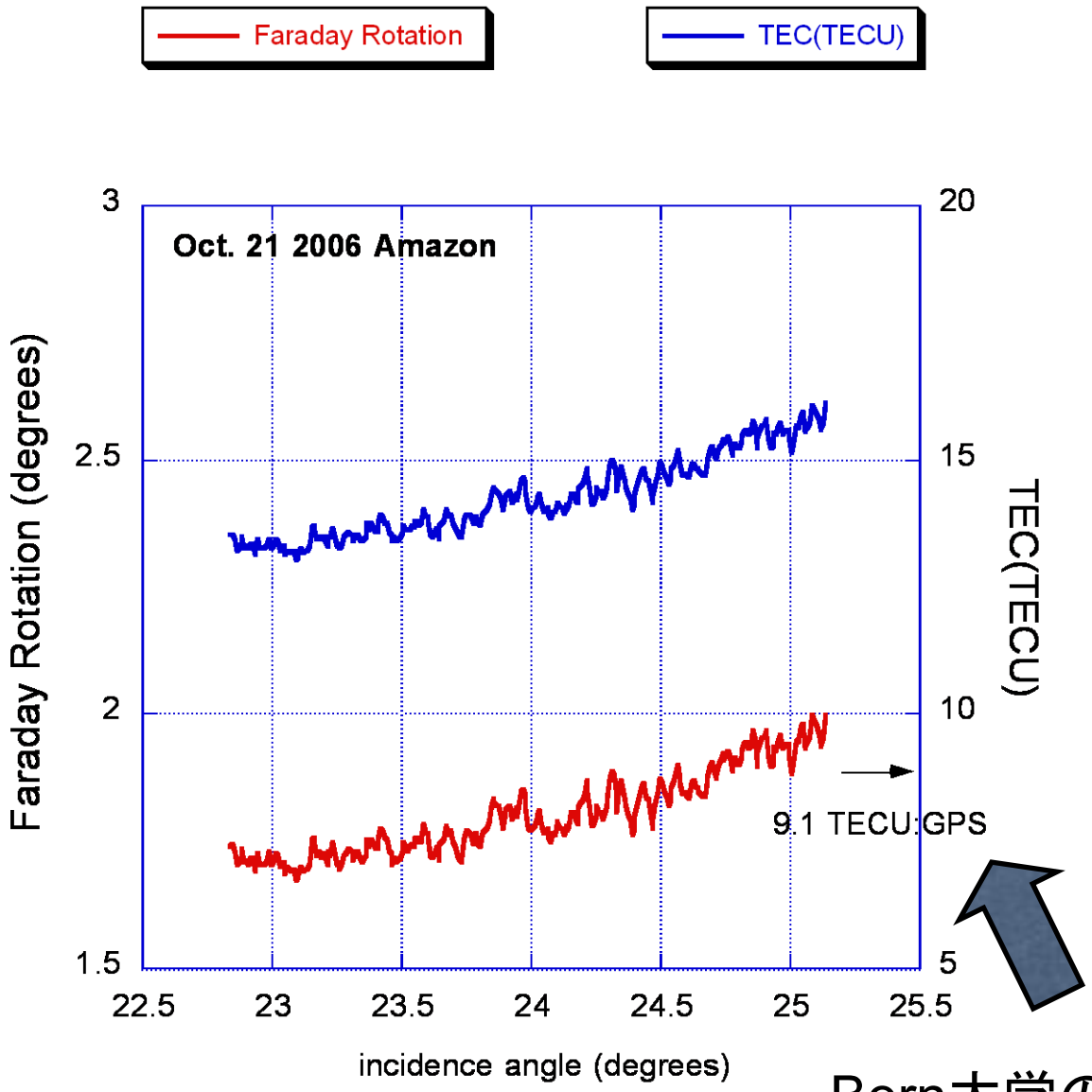

Bern大学のサイトより

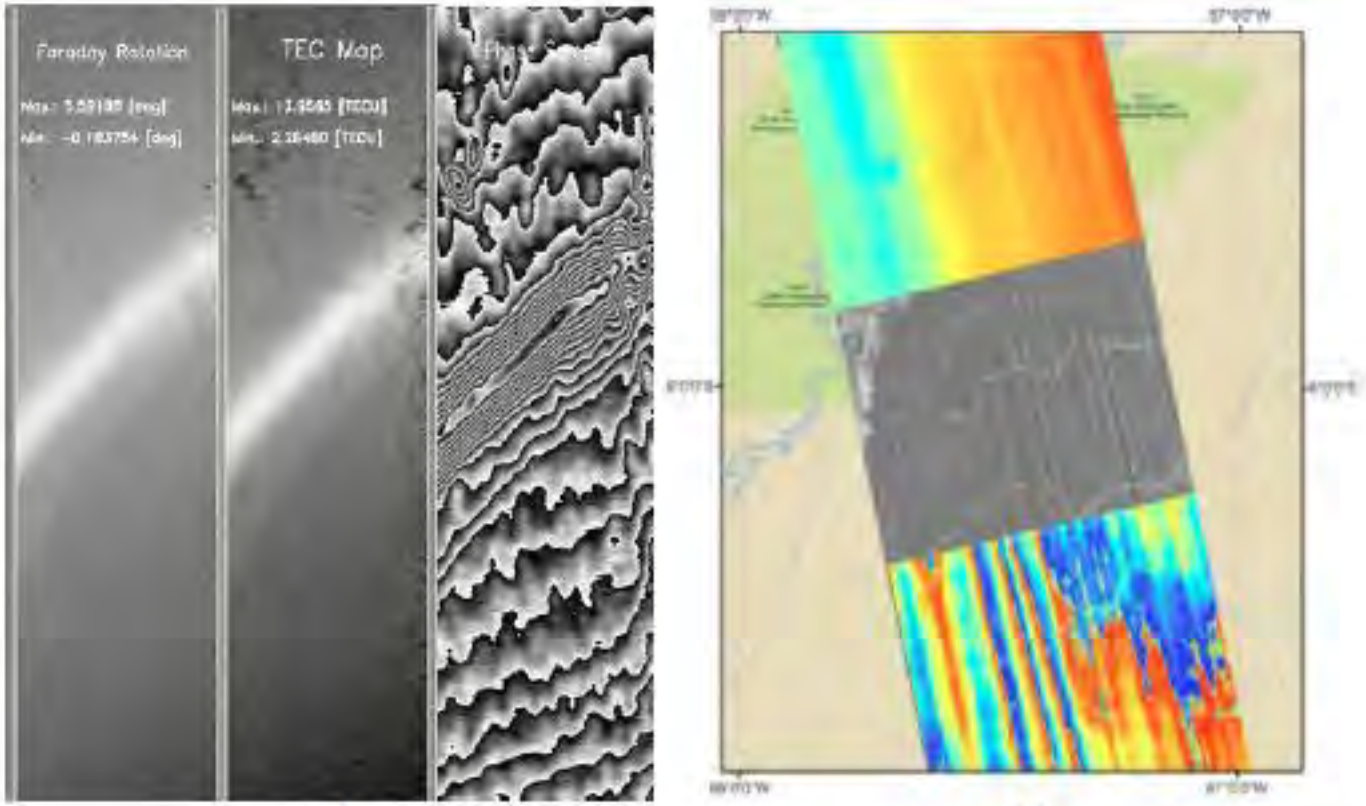

a) b)

Figure 1: a) Example of ionospheric effects caused by aurora activity in sub-arctic regions (l.t.r.: Faraday rotation estimate, derived TEC maps, predicted ionospheric phase screen); b) example of ionospheric effects caused by ionospheric bubbles in equatorial regions (top to bottom: unwrapped InSAR phase, stripes in amplitude image, ionospheric signal in wrapped InSAR phase).

F.**A review of ionospheric effects in low-frequency SAR — Signals, correction methods, and performance requirements**
Geoscience and Remote Sensing Symposium (IGARSS), 2010 IEEE International
Digital Object Identifier: 10.1109/IGARSS.2010.5654258

Causes for the stripes

Scintillation in range

Ion Density variation ：Azimuth shift

Doppler Frequency：Observation target (ionosphere) changes the Doppler frequency.

SAR received signal at intermediate frequency：

$$f(-\frac{2R}{C})$$

Time variation:

$$\frac{df}{dT} = jWf\left(-\frac{2dR/dT}{\frac{C_0}{n}} + \frac{2R}{\left(\frac{C_0}{n}\right)^2}\left(n^2\right)dn/dT\right)$$

Doppler

Doppler by media → Shift in azimuth

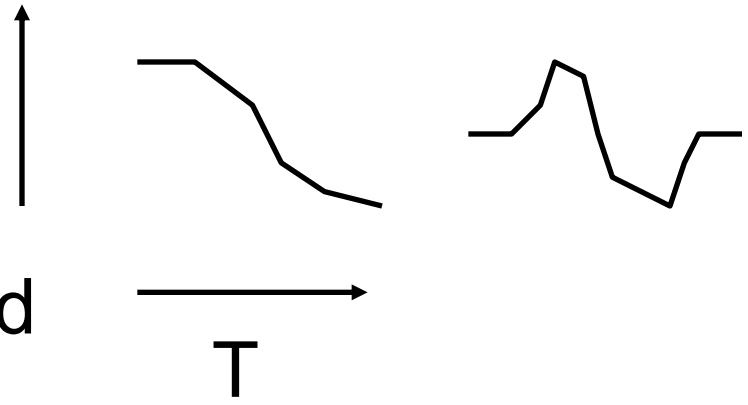

n:electron density

$n(T - V_pT)$

Shift in Az and rg

$$df / dT = df / d(-2R / C) \times d(-2R / C) / dT$$

$$= f' \left(-\frac{2R'}{C} + \frac{2R}{C^2}\frac{dC}{dT} \right)$$

$$= jWf \times \left(-\frac{2R'}{nC_0} + \frac{2R}{n^2 C}\frac{dn}{dT} \right)$$

$$= jWf \times \left(-\frac{2R'}{nC_0} + \frac{2R}{n^2 C}\frac{dn}{dT} \right)$$

$$= jWf \times \left(-\frac{2R'}{nC_0} + \frac{2R}{n^2 C}\frac{-e^2}{2e^0 W^2 m}\frac{dN}{dT} \right)$$

$$n = \sqrt{1 - \frac{Ne^2}{e_0 W^2 m}}$$

$$f_{de} = f_0 \times \left(\frac{2R}{n^2 C}\frac{-e^2}{2e^0 W^2 m}\frac{dN}{dT} \right)$$

Doppler frequency due to the media variation in azimuth

Electron density distribution

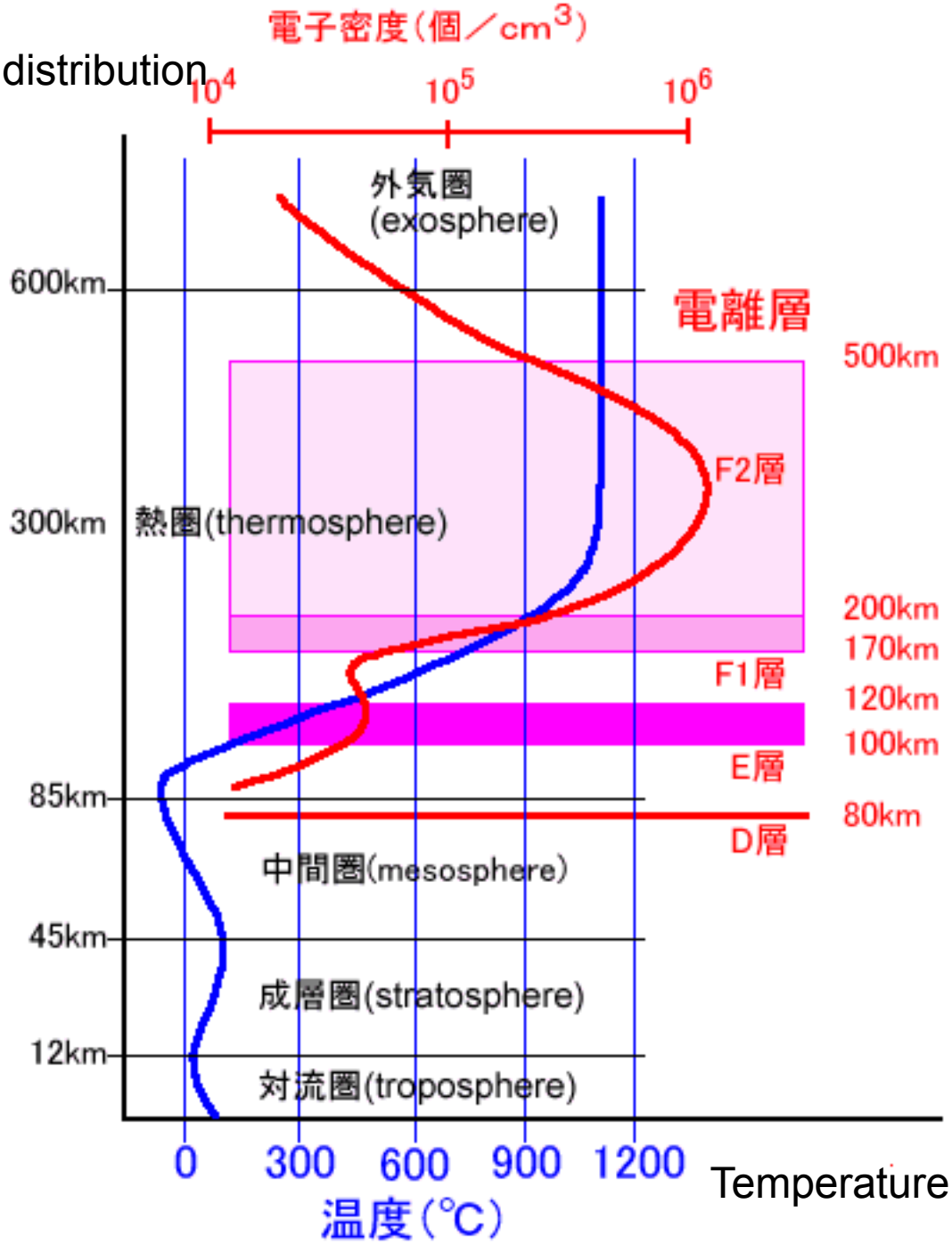

Representative parameters for the ionosphere:
Electron mass (m): 9.109e-31kg
Electric charge (e): 1.602e-19 Coulomb
Emissivity at space (e_0): 8.854e-12Fm-1
Light speed (c):299792458m-1s-1
Angular speed (ω):2*PAI*1.27e9s-1

If we assume that dN/dT~1.0e9/m^3s-1, f_{de}~0.2Hz at the positive slope and -0.2Hz at the negative slope. It vibrates in azimuth.

Change in Doppler -> Azimuth shift mainly very slightly in range.

$$Dy = \frac{Df_D}{- f_{DD}} v_g$$

Δf	:	Δy
1Hz	:	13m
0.2Hz	:	2.6m

f_{DD}=-500Hz/s
V_g=6.7km/s

Geometric evaluation using the corner reflector.

CRs in Amazon are used for the location shift and the resolution.

Geolocation

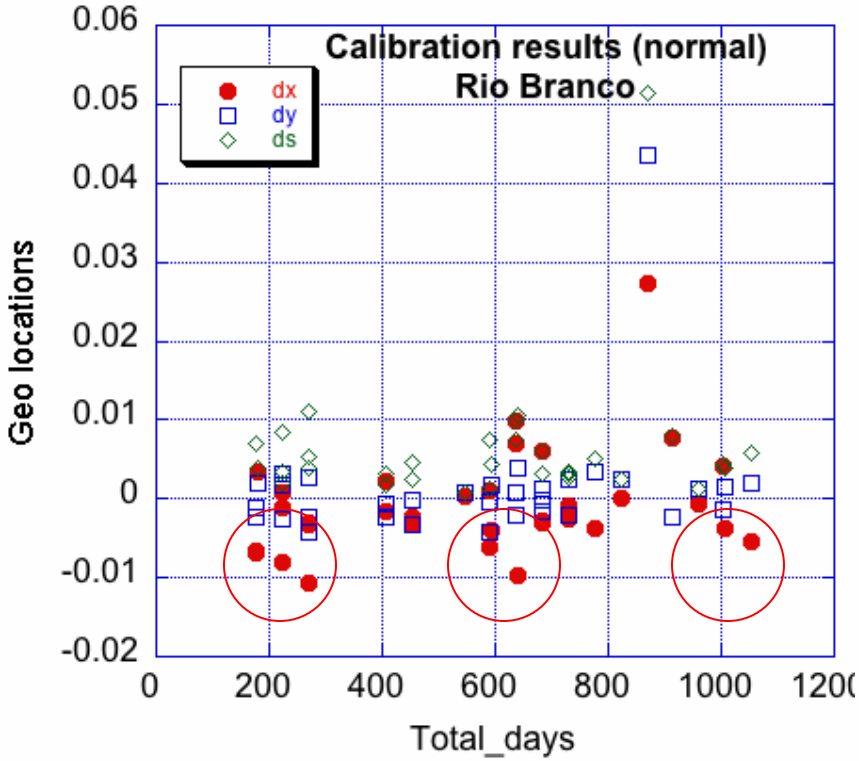

2006/w 2007/w 2008/w

Resolution

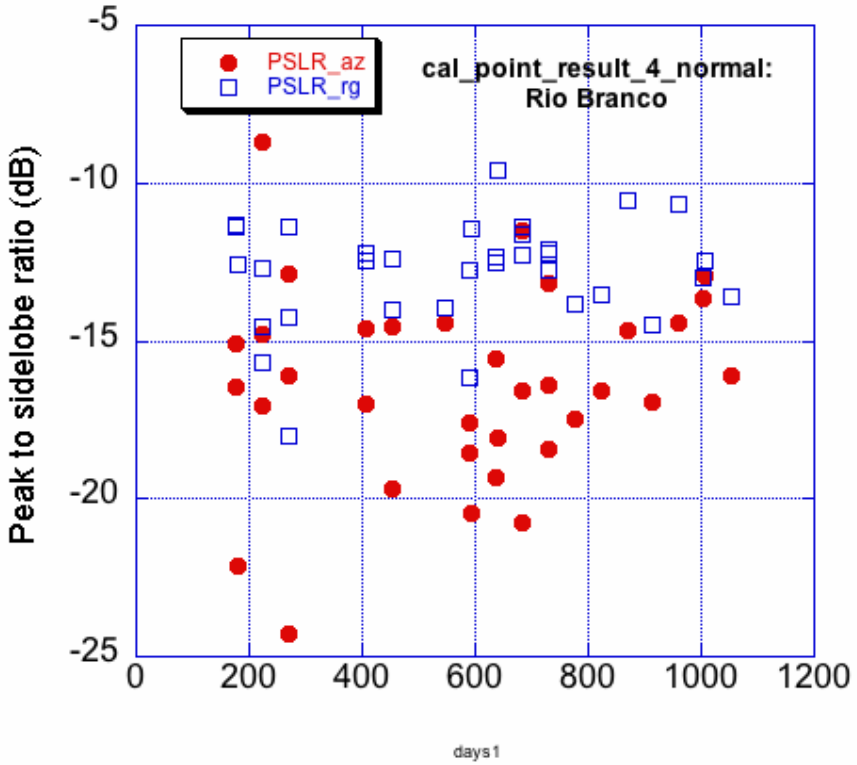

Azimuth and Range shifts

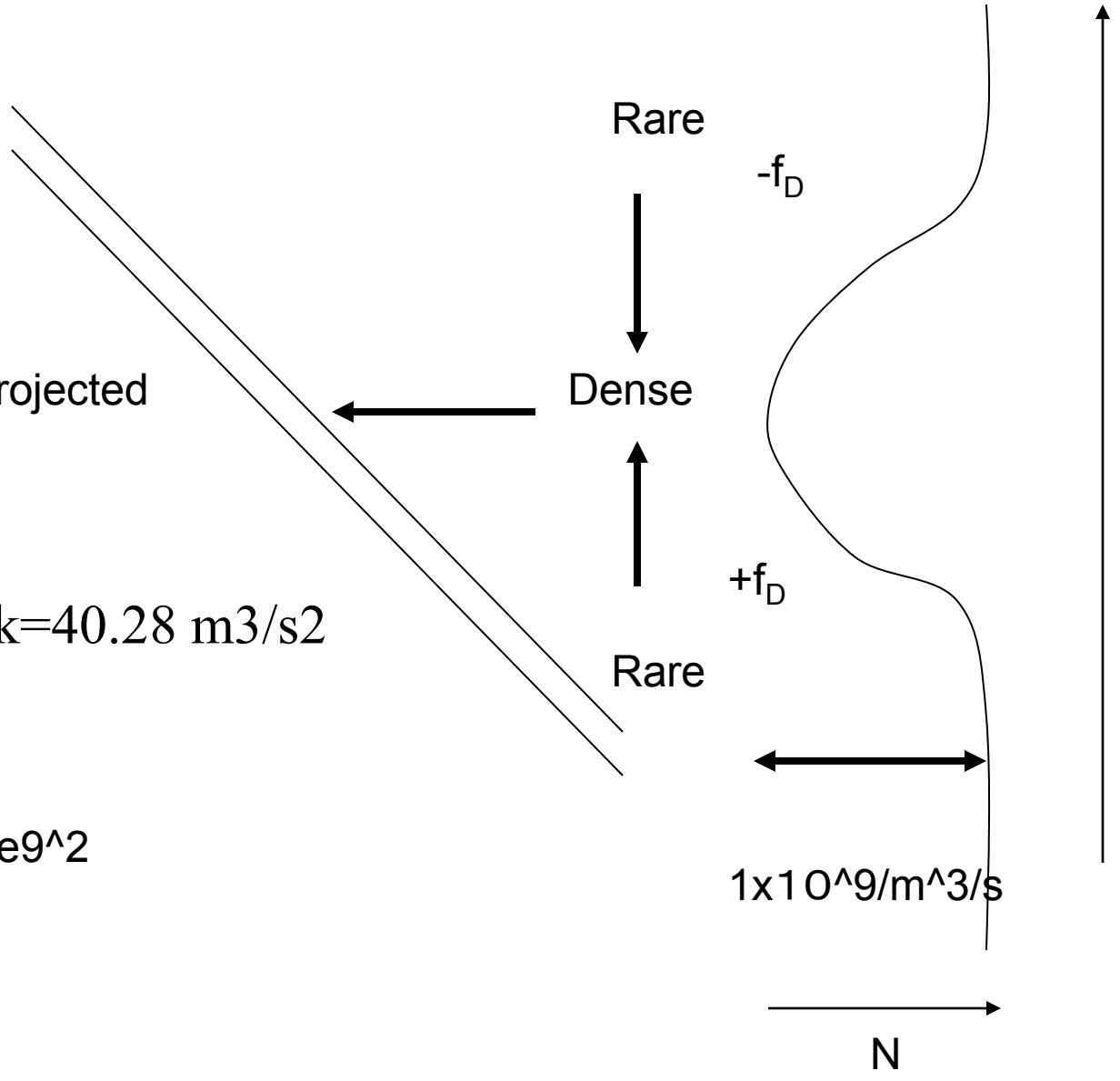

Smaller TEC, slower C, projected nearer

$$dr = \frac{k}{f^2} \mathrm{D}TEC$$

k=40.28 m3/s2

10^9*500000*40.28/1.27e9^2
=12.4m

SAR and Scintillation

SAR imaging (azimuth compression) is not affected by the scintillation

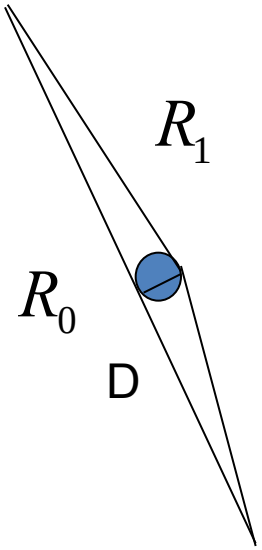

θ=23.4568 degrees

N	D
1	191.3
2	270.7
3	331.5

$$2R_0 = 2R_1 + nl$$

$$D = \sqrt{\frac{nl\left(H - z\right)z}{H\cos q}}$$

$$q = \cos^{-1}\left\{\frac{\left(H - z\right)z}{H}\frac{nl}{D^2}\right\}$$

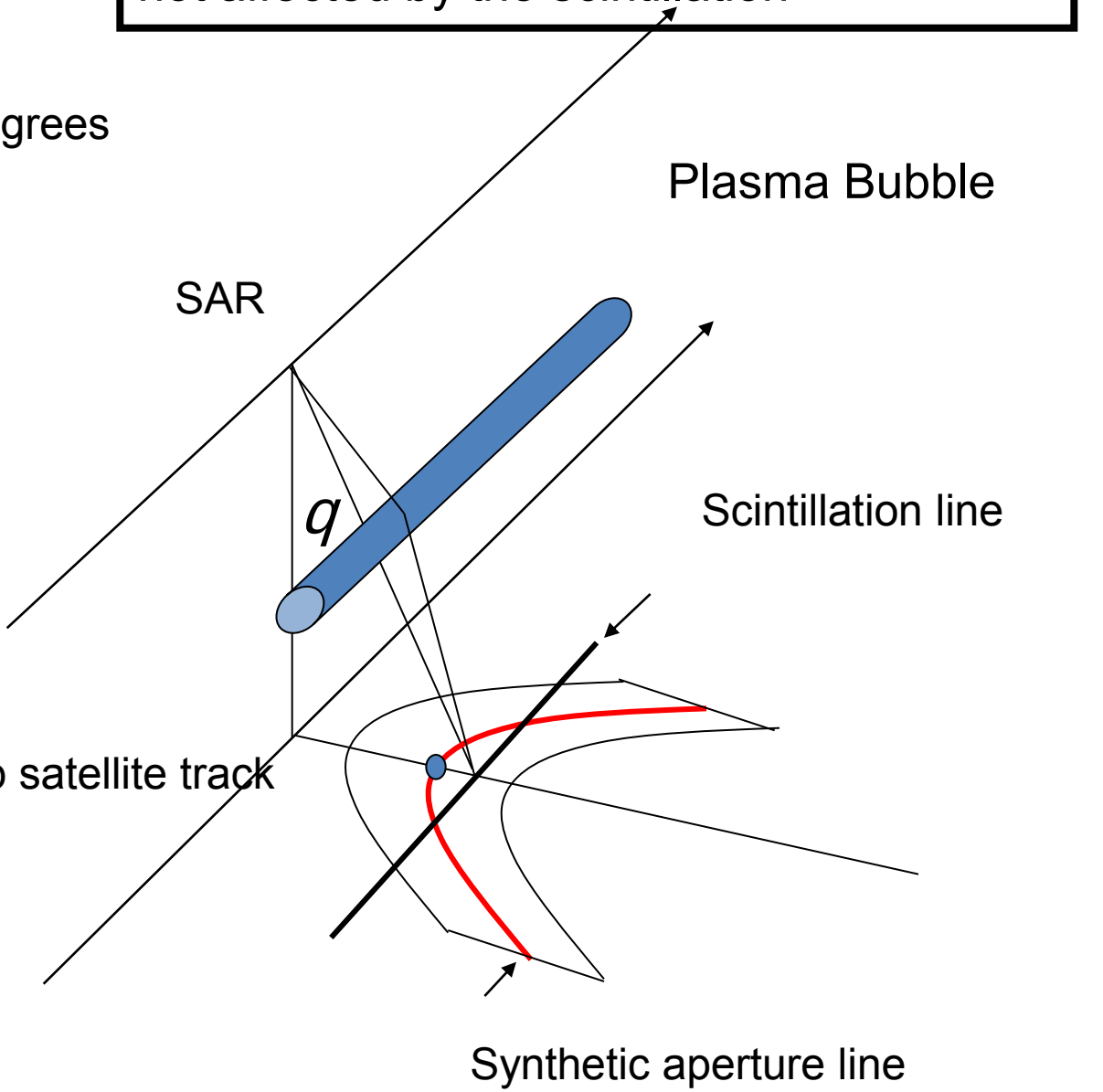

Simulation: Ranging

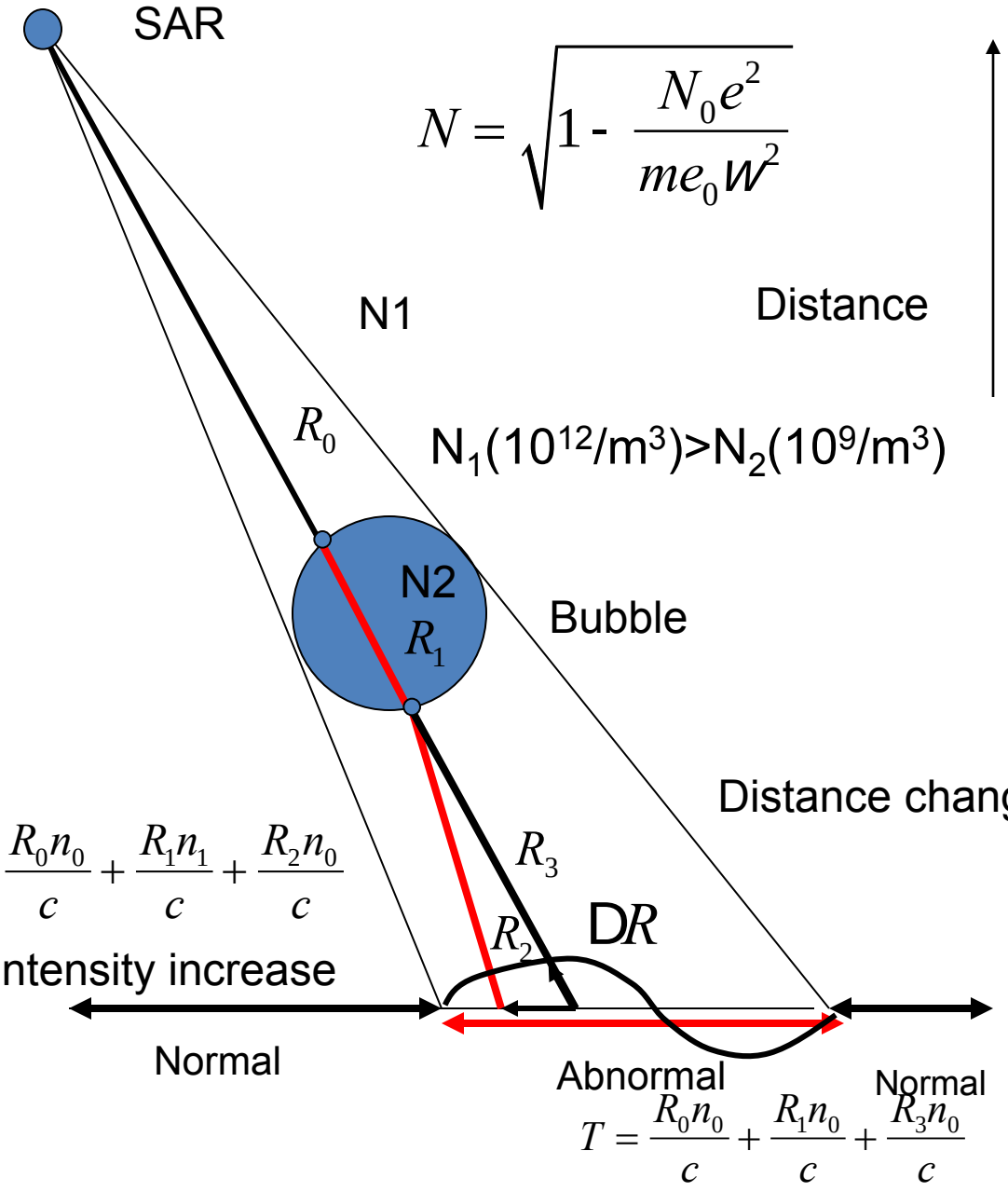

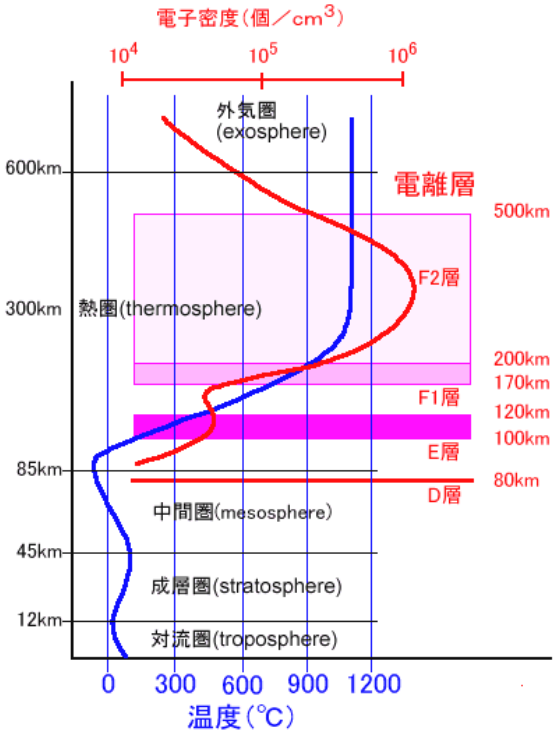

Assumption on the electron density distribution in the bubble

Case1 : Density jump in the ellipsoid

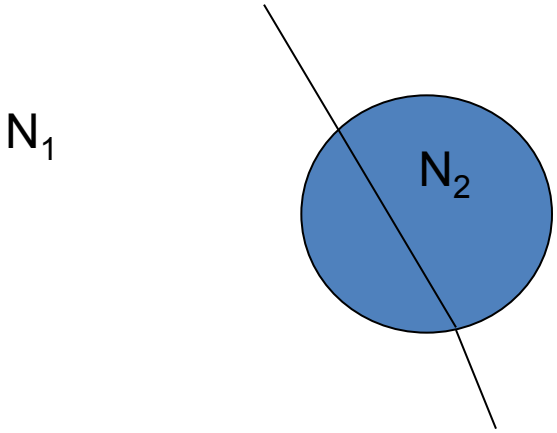

Case2 : radius dependent density distribution in the ellipsoid

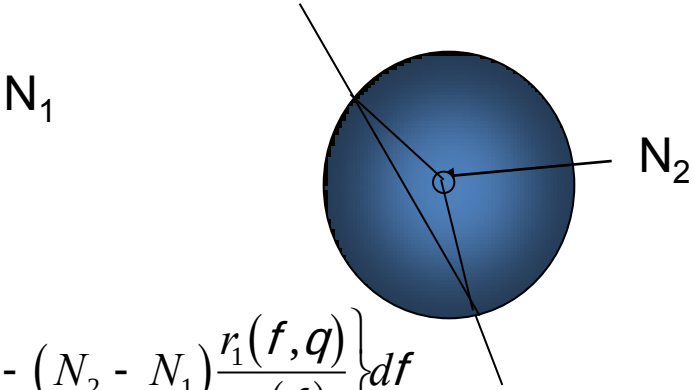

$$\bar{N} = \frac{1}{f_2 - f_1} \int_{f_1}^{f_2} \left\{ N_2 - (N_2 - N_1) \frac{r_1(f,q)}{r_0(f)} \right\} df$$

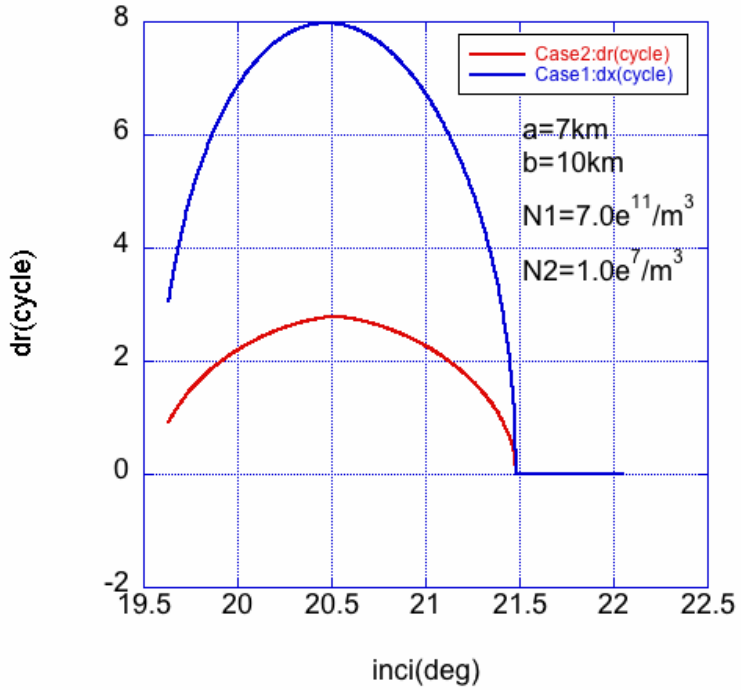

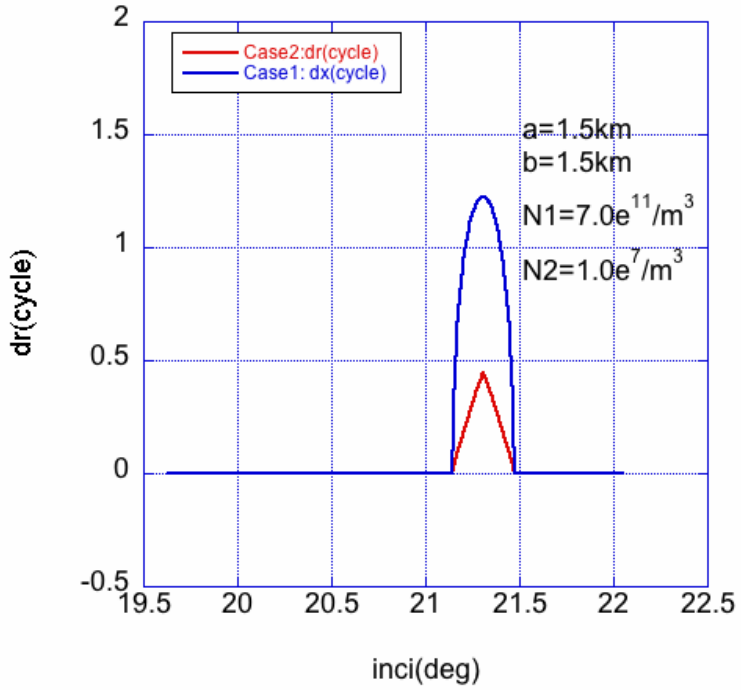

Geomagnetic lines

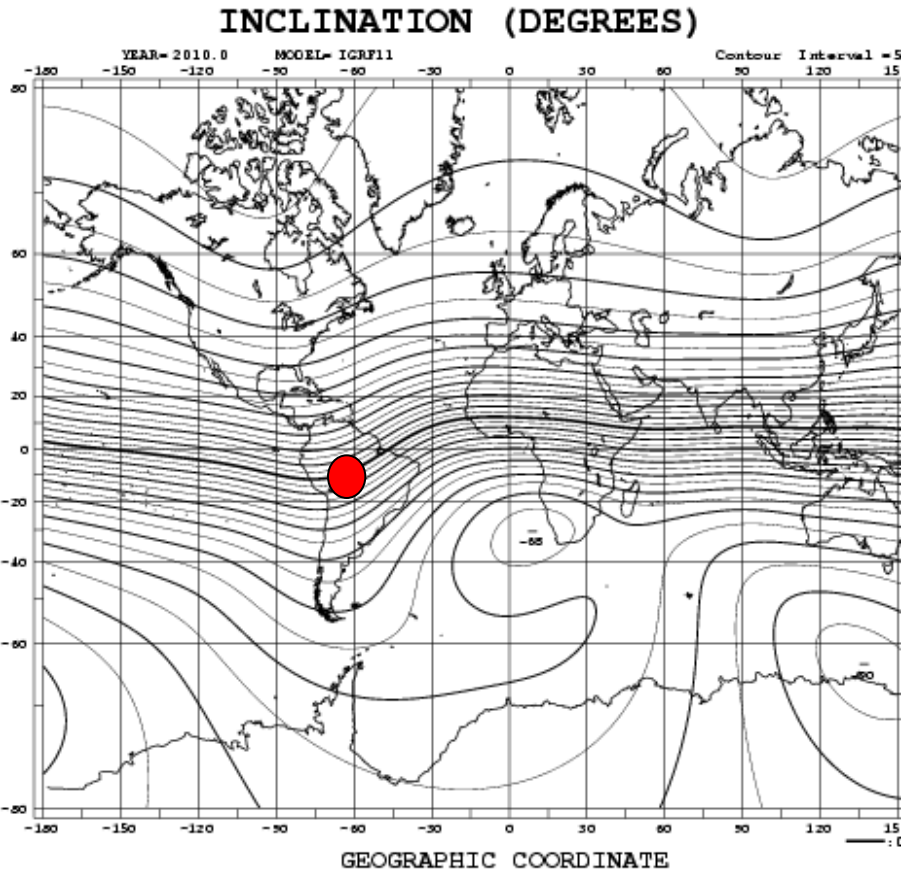

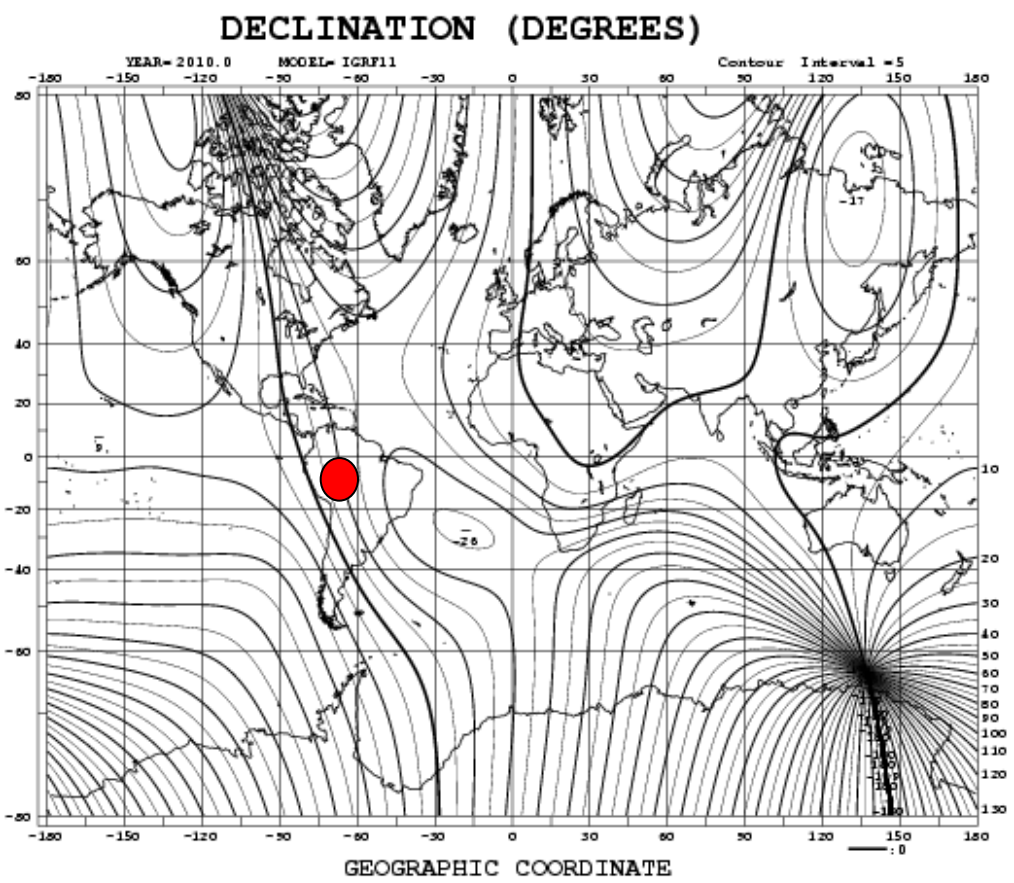

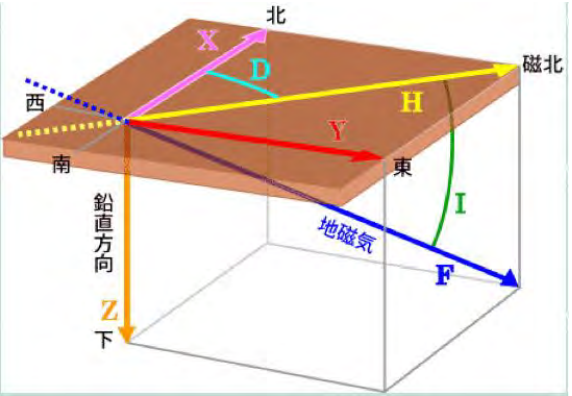

Inclination

14.79 degrees

Declination=-14.185 deg.

Comparison of the density variations on N1 and N2

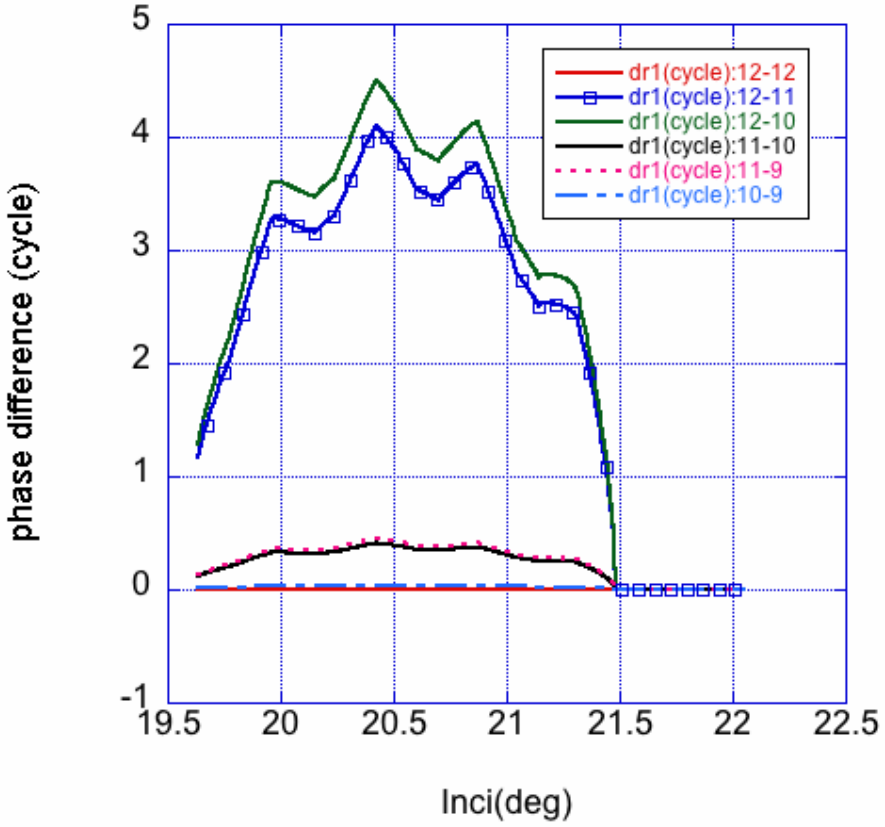

N_1 \ N_2	10^{11}	10^{10}	10^{9}
10^{12}	○	○	×
10^{11}		×	
10^{10}			×

a = 7km+1.5kmx3
b = 10km+1.5kmx3

Difference of the electron density should be at least 10^12~10^11.

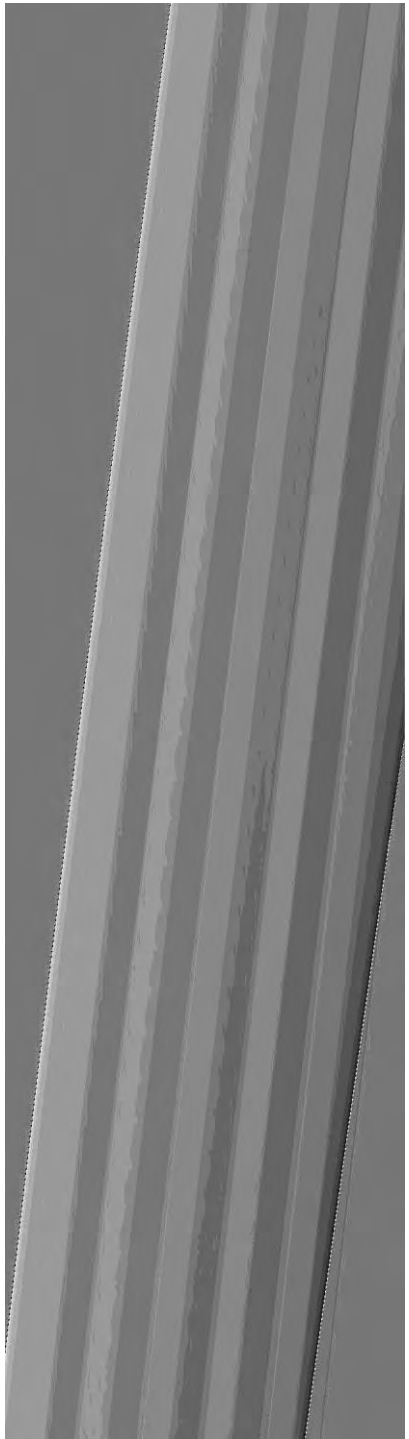

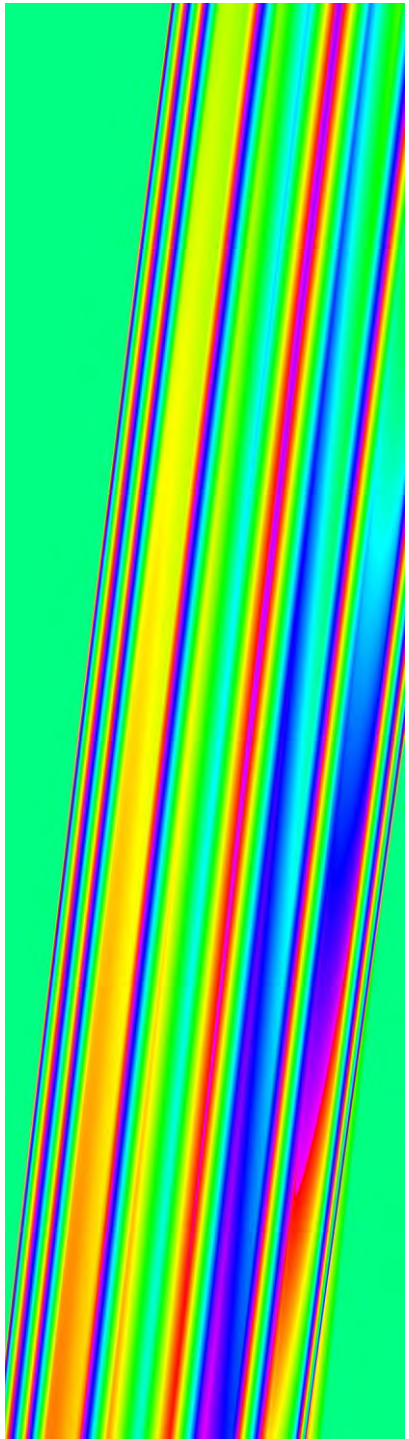

Simulated image for the Amazon case

Electron density model: case2

Inclination: 14.79 degrees
Declination:-14.185 degrees

Number of bubbles:
1 large + 4 smalls

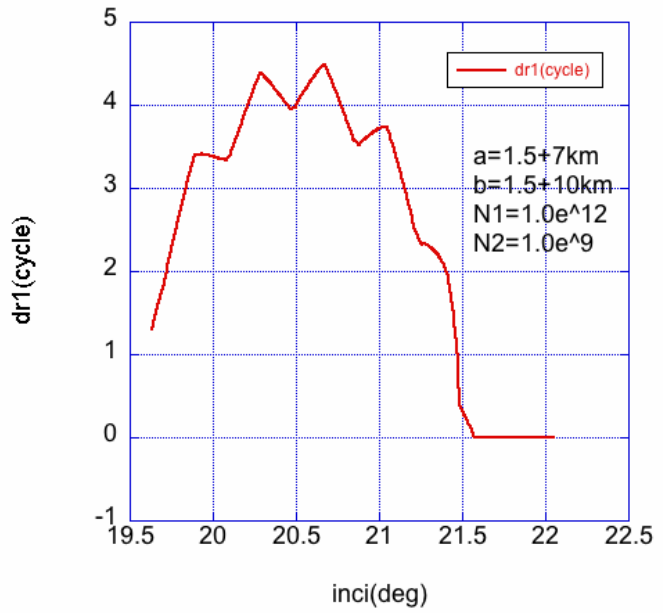

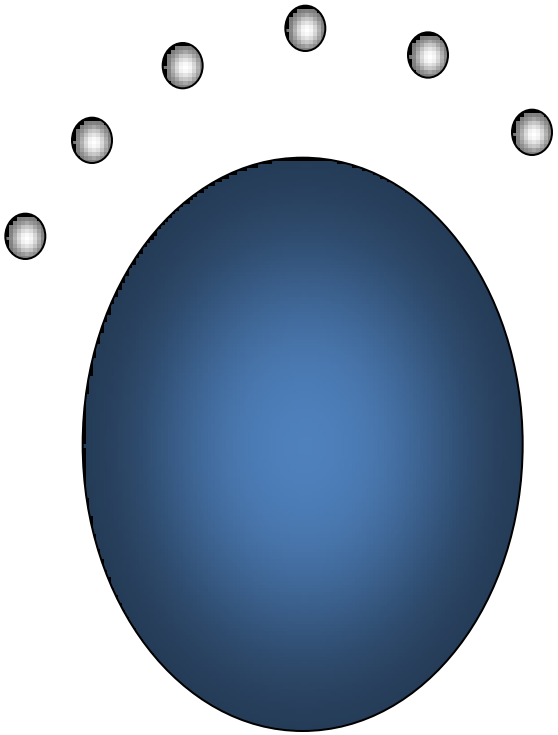

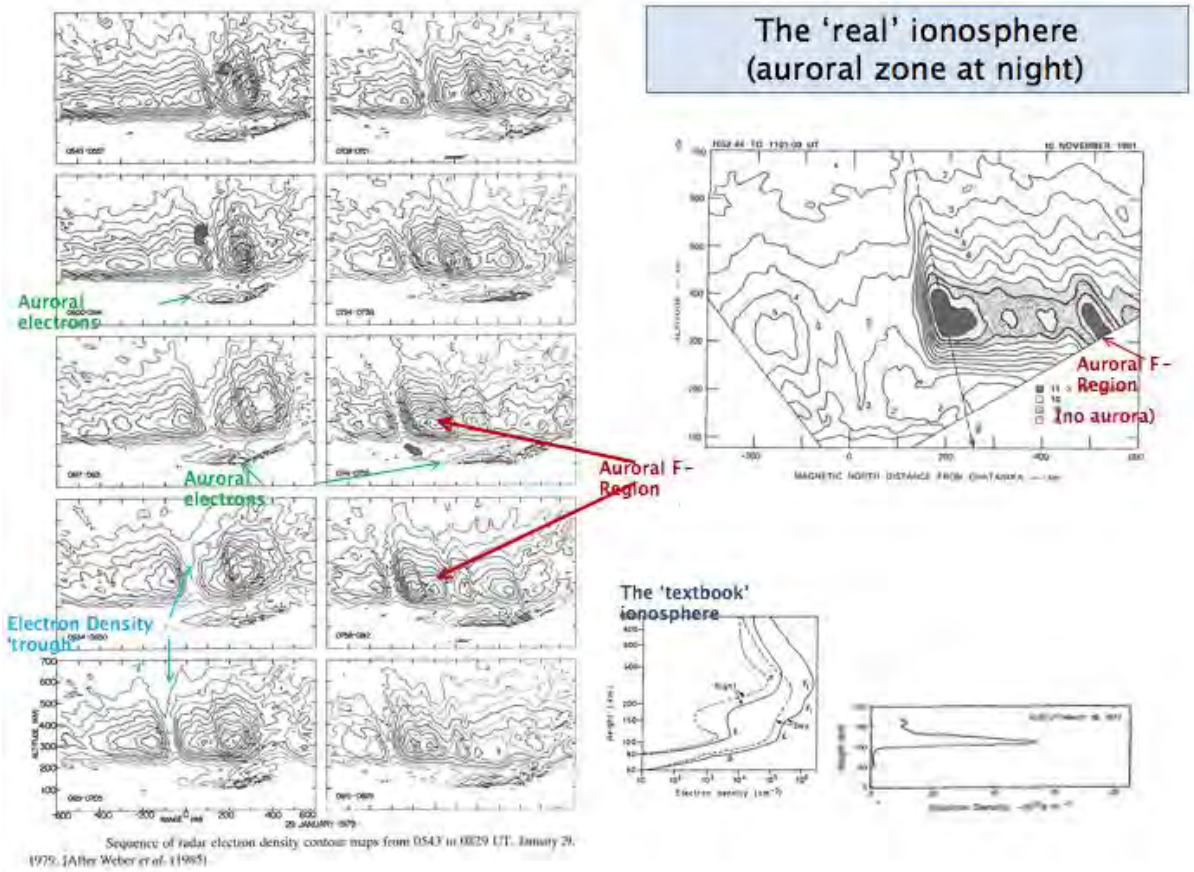

Measured cross section of the electron density
Prof. Watkins at IGARSS2009

Modelによる解法

- 相当大変：IGARSS2013 でF. Meyerに期待がかかったが、成功例の話はでなかった（残念）

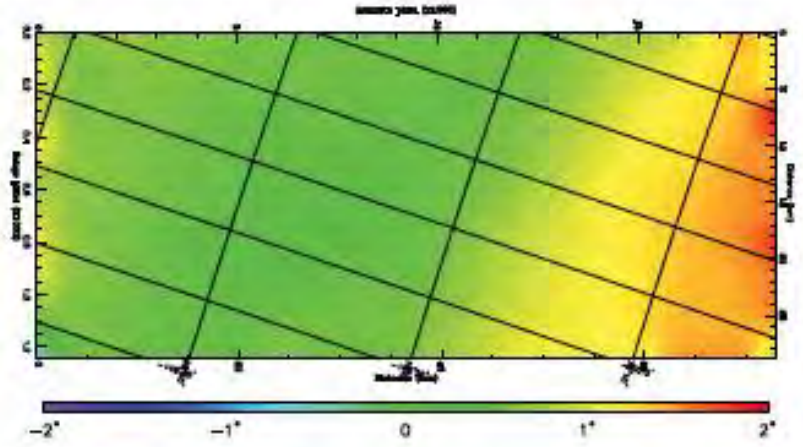

Fig. 2. Estimated differential Faraday rotation using Bickel & Bates esitmator

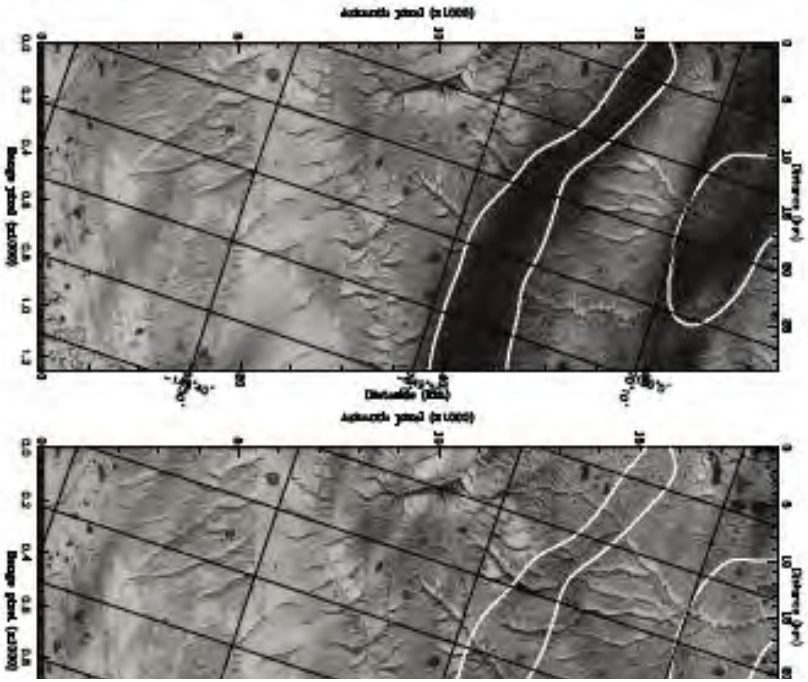

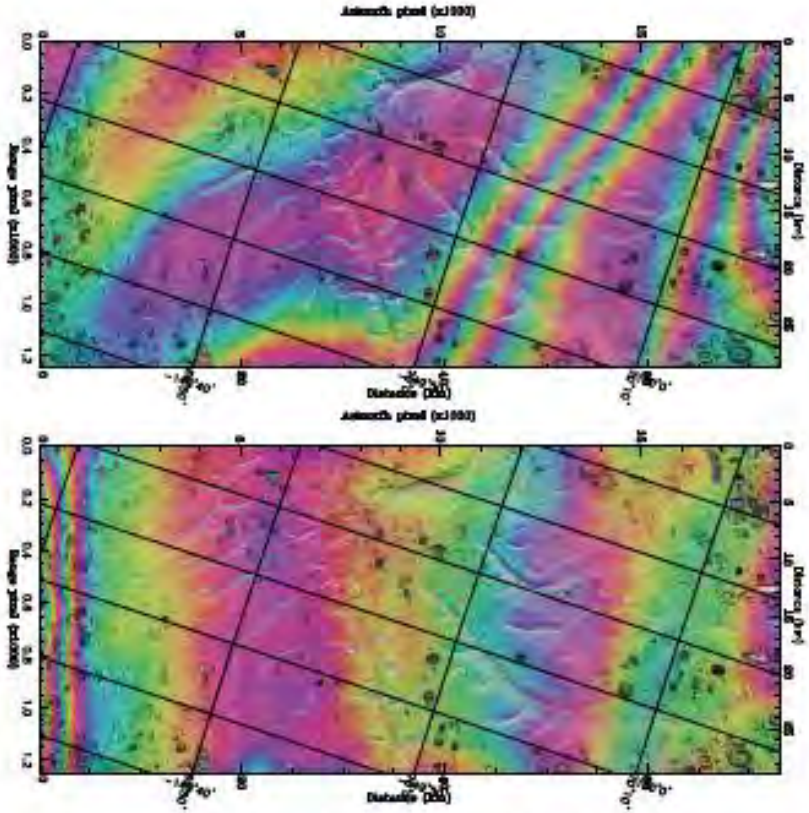

Fig. 4. Comparison of the interferometric phases, before and after correction using $\Delta\Omega$

The correlation of the master and slave images can provide the amount of misregistration, and this mismatch can be corrected by resampling the slave image. Fig. 3 shows the improvement of γ before and after the slave resampling according to the estimated azimuth offsets induced by the (differential) ionosphere. The lost of γ where TEC changes rapidly (in the white contours) is almost fully recovered.

Correction of ionospheric distortions in low frequency interferometric SAR data

Jun Su Kim; Danklmayer, A.; Papathanassiou, K.; IGARSS), 2011 IEEE International

代表的な論文

Meyer, F.**A review of ionospheric effects in low-frequency SAR — Signals, correction methods, and performance requirements**
Geoscience and Remote Sensing Symposium (IGARSS), 2010 IEEE International
Digital Object Identifier: 10.1109/IGARSS.2010.5654258
Publication Year: 2010 , Page(s): 29 – 32

Measurement and mitigation of the ionosphere in L-band Interferometric SAR data
Rosen, P.A.; Hensley, S.; Chen, C.
Radar Conference, 2010 IEEE
Digital Object Identifier: 10.1109/RADAR.2010.5494385
Publication Year: 2010 , Page(s): 1459 – 1463

Correction of ionospheric distortions in low frequency interferometric SAR data
Jun Su Kim; Danklmayer, A.; Papathanassiou, K.; IGARSS), 2011 IEEE International
Page(s): 1505 - 1508
Digital Object Identifier: 10.1109/IGARSS.2011.6049353

まとめ及び将来の展望

- 厄介な問題である。
- 唯一FRだけが解決されている。
- 解決方法はまだ定まっていない。

- ＞PALSAR-2 の85MHzは希望かも。